BNL-96142-2011-JA

DESIGN OF A SHADOWBAND SPECTRAL RADIOMETER FOR THE RETRIEVAL OF THIN CLOUD OPTICAL DEPTH, LIQUID WATER PATH, AND THE EFFECTIVE RADIUS

M. J. Bartholomew*, R. M. Reynolds[+], A. M. Vogelmann*, Q. Min^,
R. Edwards*, and S. Smith*
**Brookhaven National Laboratory, Upton, NY*
[+] *Remote Measurements and Research Company, Seattle, WA*
^*State University of New York, Albany*

Accepted for publication in
Journal of Atmospheric and Oceanic Technology

May 2011

Atmospheric Sciences Division/Environmental Sciences Dept.

Brookhaven National Laboratory

U.S. Department of Energy
Office of Science

DISCLAIMER

Abstract

The design and operation of a Thin-Cloud Rotating Shadowband Radiometer (TCRSR) described here was used to measure the radiative intensity of the solar aureole and enable the simultaneous retrieval of cloud optical depth, drop effective radius, and liquid water path. The instrument consists of photodiode sensors positioned beneath two narrow, metal bands that occult the sun by moving alternately from horizon to horizon. Measurements from the narrowband 415-nm channel were used to demonstrate a retrieval of the cloud properties of interest. With the proven operation of the relatively inexpensive TCRSR instrument, we discuss how it may also be useful for retrieving aerosol properties under cloud-free skies, and for ship-based observations.

1. Introduction

Thin clouds for the purposes of the paper are defined as warm clouds with liquid water path (LWP) ≤ 100 gm^{-2}, which have a critical impact on radiative transfer within the atmosphere and hence on Earth's radiative energy balance (Turner et al. 2007b). Such clouds are abundant and, from the tropics to the Arctic, 50% or more of the liquid-water clouds have LWP < 100 gm^{-2} (Marchland et al. 2003; Turner et al. 2007a; Turner et al. 2007b). The shortwave radiative fluxes of clouds are very sensitive to small changes in the LWP when the LWP is small (Sengupta et al. 2003), which requires a particularly high degree of accuracy from observations and modeling. For example, an uncertainty of $\pm$ 20 gm^{-2} in LWP can translate to $\pm$ 150 Wm^{-2} in downwelling surface flux (Sengupta et al. 2003; Min and Duan 2005; Turner et al. 2007b). The common occurrence of thin clouds necessitates that we develop new methods, such as the one discussed here, that can observe their properties to within the accuracies needed for climate and numerical weather prediction applications.

Three of the most fundamental cloud properties that dictate their impact on the Earth's energy budget are cloud optical depth (COD), drop effective radius (Re; Hansen and Travis 1974), and LWP. For cloud-drop-sized particles at visible wavelengths, these properties are related as

$$\mathrm{COD} \approx 3\,\mathrm{LWP} / (2\,\rho\,\mathrm{Re})$$

where ρ is the density of water. Hence any method that adequately retrieves two of the three factors provides the information needed to determine the third. The third property, however, is the least well determined as its uncertainty includes the combined uncertainties of the other two terms. A number of instruments and techniques have been previously used to observe cloud properties and have also been applied to thin clouds; however, thin clouds require accuracies that strain the capabilities of traditional detectors (e.g., microwave receivers) and theoretical

approaches such that no single device has proven to be capable to determine all three critical properties for LWP < 100 gm^{-2} (Turner et al. 2007b). For example, micropulse lidars (MPL) and microwave radiometers (MWR) are instruments that have been commonly used for surface retrievals and satellite validation. MPL observations can provide COD for clouds up to about 3 (LWP < 25 gm^{-2}), but the signal saturates beyond that point and does not offer information on Re or LWP. Dual-channel MWRs, operating at 23 and 30 GHz, are a commonly used in the field and perform well for optically thick clouds (in absence of surface precipitation); however, uncertainties in their LWP retrievals are typically 20 to 30gm^{-2} (Liljegren and Lesht 1996; Westwater et al. 2001; Marchland et al. 2003; Crewell and Löhnert 2003), which are unacceptably large for clouds with LWP < 100 gm^{-2}. For example, an uncertainty of 20 gm^{-2} in the LWP can lead to an uncertainty of 150 Wm^{-2} in downwelling surface shortwave radiation when LWP is small (Min and Duan 2005). Turner et al. (2007b; Table 2) provides a summary of many techniques used for the retrieval of microphyiscal properties of thin clouds as well as a discussion of emerging capabilities that may provide additional sensitivities.

In the case when the sun is obscured by a thin cloud, a solar aureole is presented that offers a means to simultaneously retrieve the three critical cloud properties (COD, Re, and LWP) across the thin-cloud range (up to 100 gm^{-2}) using a single, relatively simple instrument. The solar aureole is the region of enhanced brightness around the solar disk, which is caused by the forward scattering of particles that are much larger than the wavelength of incident radiation (*i.e.*, are diffracted). Under thin clouds, the radiant intensity of the solar aureole gradually decreases away from the solar disk, with the greatest decrease occurring within about the first 5° and tapering off by 15° (e.g., Min and Duan 2005). The aureole shape (change of intensity with angle away from the center of the solar disk) depends on the COD and particle size distribution (Min et al. 2004; Min and Duan 2005). For example, for a fixed COD, larger particles enhance

the scattering in the forward direction, thereby concentrating greater intensities at the smaller angles. Mie theory can be used to calculate the single scattering behavior of cloud drops. Furthermore, the calculations can be simplified by the use of Re even though water clouds contain a distribution of drop sizes (Hansen and Travis 1974; Hu and Stamnes 1993). Since the solar disk is present up to a COD of about 10 (Bohren et al. 1995), such an observational approach could potentially span, using one technique, the lower limit of optical depths (and LWP) that is problematic for other current approaches.

Although exploiting the solar aureole has been used for retrieving aerosol optical depth and size distributions (Nakajima, et al. 1983; Kaufman et al. 1994, Dubovik and King 2000), relatively few studies have exploited it to retrieve cloud properties. Imaging methods, using charge-coupled device (CCD)-based sensors with sun tracking or manual pointing, have been used to characterize the solar aureole under cloudy conditions (Ritter and Voss 2000; DeVore et al. 2009). A benefit of such methods is that the CCD array can measure the brightness for the entire two-dimensional disk of the aureole, which enables redundant measurements of intensity across the aureole (*i.e.*, diameter transects) that can be averaged to improve the signal to noise ratio. For routine observations, such systems require some sophistication to manage the potentially challenging photometric calibration issues of the CCD array, and manage the automated orientation of the CCD array towards the sun. Sun trackers can perform such orientation, but add complexity and may be impractical if performed on a moving platform such as a ship.

This paper describes the Thin-Cloud Rotating Shadowband Radiometer (TCRSR), which is a new application of shadowband radiometry for observing the solar aureole, as proposed by Min and Duan (2005). The instrument design builds upon previous advancements in monitoring surface solar radiation. The heritage of the TCRSR is discussed, and modifications are described

to meet the desired specifications of the solar aureole measurements. Initial deployments are presented, which demonstrates the capabilities of the system and provides examples of retrieved cloud microphysical properties. The paper concludes with a summary and a discussion for how the device could be used or modified for routine observations of cloud and aerosol properties, including the potential for making observations from moving platforms.

2. Instrument Design and Testing

Calculations by Min and Duan (2005) find that for thin clouds (optical depth < 10) retrievals using the solar aureole can attain accuracies in optical depth, Re and LWP, respectively, of 2%, 10% and 2 gm^{-2}. The desired measurements of the solar aureole can be obtained (based on Min and Daun 2005) by an instrument with a shadowband that occults 2° of the sky with 1° resolution across the aureole (*i.e.*, within ± 15° of the sun's disk). The design and operation of a TCRSR meeting these requirements are described here.

a) Hardware Description

The fundamental design of the TCRSR comes from two earlier instruments – the Multi-Filter Rotating Shadowband Radiometer (MFRSR), and the Fast Rotating Shadowband Radiometer (FRSR). The MFRSR (Harrison et al. 1994) makes spectral irradiance measurements from a fixed platform and its measurement protocol calls for occulted and non-occulted observations of the sun with a shadowband that is 3.27º wide. The diffuse horizontal and total horizontal solar irradiances are observed from which the direct-normal irradiance can also be determined. The sensor head, which contains seven photodiode detectors positioned under a diffuser, measures the solar irradiance with a broadband channel (0.3 to 1.1 μm) and six narrowband channels each approximately 10-nm wide. The nominal central wavelengths are 415, 500, 615, 673, 870 and 940 nm. The MFRSR partitioning between direct and diffuse irradiance is determined from measurements made with a shadowband (occulter) positioned at four discrete locations. Two

observations are made with the MFRSR shadowband 9º from the sun; one observation is made with the sun completely occulted, and one is made with the sky and sun completely unocculted.

The TCRSR is closer in design to the FRSR (Reynolds et al. 2001) that was designed to make observations from which the direct-normal spectral irradiance could be determined even from moving platforms such as ships at sea. To enable measurements from a moving platform, the FRSR instead makes 250 continuous measurements over the upward hemisphere as a direct-current (DC) motor propels the shadowband 360° around a horizontal axis centered on the sensor head. A full FRSR sweep takes approximately seven seconds, and all seven channels are collected simultaneously. The shadowband is wide enough that the sun is fully occulted at some point during the sweep, which depends upon the sun's position and the ship's heading, pitch and roll. A desktop computer provides instrument control and collects the data from the sweep, which includes the sweep irradiances, location, time, and the platform pitch and roll. An advantage of the continuously operating FRSR (and TCRSR) method is the ability to characterize the whole upper hemisphere sweep, which allows better separation of the direct irradiance from the diffuse irradiance than is possible by the discrete-angle-measurements of the MFRSR. Post-processing of the sweeps determines the depth of the shadow, which is directly related the normal spectral irradiance. Such measurements (after cloud screening) have been used to retrieve aerosol optical depth to within the accuracy needed for climate studies (Miller et al. 2004; Miller et al. 2005). The instrument has proven to be robust and 12 units have been built and deployed on ships and cruises since 1999, including three that the Japanese Agency for Marine-Earth Science and Technology has operated continuously for more than five years.

The TCRSR uses the same sensor head and general operating design as the FRSR, which enables measuring not only the depth of the shadow but also its shape. Thus, it is well suited to measure the shape of the solar aureole needed for thin-cloud retrievals, although several

modifications are needed. The TCRSR uses two rotating shadowbands: one occults 5° of the sky (standard FRSR design) and a second occults 2° (Figure 1). The 2° band is the most critical to obtaining the desired sensitivity for the cloud property retrievals. The 5° band, although less critical, is expected to help stabilize the retrievals, and can also provide a comparison to the 2° data for purpose of quality control. Since the main effort in design modification was required to accommodate the 2° band, the 5° band was included with little additional effort.

The width of the 2° band is the same as for the 5° band (0.75 inches), but it has a greater radius of rotation. Based on the calculations by Min and Duan (2005), smaller occultation angles provide more sensitivity to changes in optical depth and Re. For the prototype TCRSR, however, the larger radius was dictated by the fixed instantaneous field of view of the detectors in hand and the need for a robust mechanical structure. (While we would have preferred even a smaller occultation angle, a narrower shadowband at a smaller radius would have been too flimsy.) This combination of band width and radius seemed the most practical for band stability (*e.g.*, to vibration and wind) and required a similarly sized driving motor as with the FRSR. A pivot opposite the motor was required as well for stability of the 2° band with its large radius. This necessitated changing the sweep motion from being a continuous circle (as for the FRSR) to one that alternated back-and-forth over the upper hemisphere. The back-and-forth motion is controlled via contact switches that are used to detect the end of each sweep, and triggers the start of the next sweep. Each set of sweeps takes approximately 20 seconds (14 s for the 2° band, 7 s for the 5°); the resultant data set consists of sweeps for all seven channels for the 2° and 5° occultations. The data volume for an hour of observations per band (all six channels) is 2 MB.

b) Installation and Operations

Bench tests and initial field testing were conducted at Brookhaven National Laboratory from

July to November 2007, after which the TCRSR was deployed twice in 2008 on the roof of the radiometer calibration facility at the Atmospheric Radiation Measurement (ARM) Climate Research Facility's (ACRF's) Southern Great Plains site (Figure2), from 7-9 January and from 2-5 July. The sampling rate and shadowband sweep rate were configured with a 0.24° angular resolution, which exceeds the design specification of 1°.

The technique used for photometric calibration of the TCRSR was identical to that used for the FRSRs and MFRSRs. The electronic gains are determined from bench measurements using a precision millivolt reference for each channel. The radiometer head comes from the manufacturer (Yankee Environmental Systems, Inc.) with a linear, direct-normal irradiance gain equation for each channel in units of Wm^{-2} for the broadband channel and $W(m^2 \cdot nm)^{-1}$ for the narrowband channels. In addition, the shape of the spectral band passes and the cosine responses (incident angle sensitivities for the direct beam) were provided for each detector by the manufacturer. A more detailed discussion of the calibration method can be found in Reynolds et al. (2001).

We employ two approaches to refine the calibrations that were provided by the manufacturer. The ARM Program has the capability of characterizing the photometric gain (using standard lamps) and the cosine response, which were performed for each deployment. The gain calibrations agreed to within 5% for all narrowband channels except the 415-nm channel, which is often found to be the least stable and had only 14% agreement between calibrations. Alternatively, an asset of the shadowband technique is that the forward-scattering lobe and the total-horizontal irradiance are measured by the same detector. This allows for accurate determination of atmospheric transmittances (without absolute calibration) via Langley regression, where the direct-normal irradiance on stable, clear days can be used to extrapolate the instrument's response to top of the atmosphere (TOA). This calibration can then be applied to

the total horizontal irradiance and transmittances are calculated subsequently under all-sky conditions as the ratio of the uncalibrated signal to the extrapolated TOA value. These approaches provide the desired radiometric accuracy for retrievals, as demonstrated in Yin et al. (submitted).

3. Results

Examples of observed irradiance sweeps at 500 nm are shown in Figure 3, which focus on the irradiances within ± 5° of the sun. Each raw sweep is corrected for incidence angle sensitivity (Harrison et al. 1994). Initially, as the shadowband moves across the sky, the signal from the sensor head is the global value (unoccluded) minus the irradiance of the strip of sky that is occluded by the band. Then, as the band approaches the sun, it gradually occults more of the solar aureole gradually reducing the signal to the detectors until the whole solar disk is occulted (signal minimum). As the band continues, less of aureole is occulted and the signal rises. Compared to clear skies, the part of the sweep with reduced signal becomes broader and less sharply defined during cloud events (Figure 3). During thin-cloud events, the shape of the shoulder and dip in successive scans can be markedly different, indicating the degree of cloud variability that can be captured by the instrument within only 40 seconds (*i.e.*, two successive 2° sweeps).

The variation that is possible among successive scans is shown more clearly in Figure 4, where each scan is not normalized (as in Figure 3) and the sweep (band angle) is shown for almost the full hemisphere. This figure shows the added information content afforded by the sweep data compared to typical hemispheric diffuse field-of-view observations. Although the shapes of the successive scans are markedly different (and therefore their hemispheric diffuse fluxes are likely different), the depth and shape of the sweeps in each panel are essentially the same, suggesting that similar cloud optical properties would be retrieved from the data.

The difference of the unblocked and blocked irradiances yield the irradiance of the forward scattering lobe of the solar aureole plus the direct solar beam. The unblocked irradiance is obtained for each sweep from the maximum irradiance observed. The maximum typically occurred at the beginning or end of a sweep, but in varying cloud conditions the maximum could occur, on occasion, at other points along the sweep. Figure 5 shows the spectral fidelity of one of the scans obtained from a test period at Brookhaven National Laboratory during a fog episode. Note the small point-to-point variability relative to the signal magnitude. Naturally, this degree of variability becomes more significant for thicker clouds that have a less pronounced aureole. One way to place an upper bound on the system noise is to consider the global values during clear skies. Several samples of global irradiance were obtained at the beginning and at the end of the sweep during clear skies, when the band was horizontal and the sun overhead. The global standard deviation was typically 0.1% of the global mean, which is taken as an upper uncertainty limit. This limit is routinely seen from this instrument and, of course, the signal-to-noise ratio can be improved by averaging several sweeps.

An example of cloud property retrieval for a water cloud within a broken cloud field is shown in Figure 6. To assist retrieval stability, the difference of the unblocked and blocked irradiance is first smoothed. The shape of this difference is then compared to those from a library of simulations, and the retrieval uses the optical depth and Re from the simulation that best matches the observation (for details, see Yin et al. submitted). Generally speaking, the maximum of the difference is largely dictated by optical depth and the width by Re. For the case shown, the retrieved optical depth and Re are, respectively, 1.8 and 8 μm. These results are preliminary, and verification of the retrieval technique is the topic of further research (Yin et al. submitted).

4. Concluding Remarks

The TCRSR was developed to make observations of the sun's aureole caused by thin clouds. These observations can be used to simultaneously retrieve COD, Re and LWP for thin, warm clouds, which are an important for climate studies. For future applications of this design, it should be noted that a successful observation does not require absolute accuracy in the band-angle position for each sweep, since the minimum of observed scans enable registering the band position against the sun position and can account for any angular biases. However, knowing the exact position of the band angle relative to the center of the aureole is crucial, since it determines the shape of the solar aureole and, thus, the accuracy of the inferred Re and LWP.

Our results demonstrate a successful, relatively simple instrument for a terrestrial deployment. While we have focused on applications to retrieving cloud properties, this type of aureole information may also be used to infer aerosol properties under clear-sky conditions (e.g., Nakijima et al. 1983). Specifically, relative to aerosol retrievals typically done using spectral sun photometer measurements, the aureole information provides the means to characterize the fine and coarse particle modes. Further, this aureole information provides a better means to separate the direct and diffuse components that may lead to improved retrievals of aerosol optical depth.

Finally, the simplicity of the design might also make it suitable for marine deployments. Such observations may be of particular interest given that marine boundary layer clouds are very important to climate and are often "thin" (*i.e.*, LWP < 100 gm^{-2}; e.g., Turner et al. 2007). Ship-based measurements would be slightly more complicated because the platform attitude must be measured (i.e., pitch, roll and heading). Such observations were routinely made as part of the FRSR design and, in theory, could be applied to the TCRSR design.

5. Acknowledgments

We would like to acknowledge the excellent and professional help provided by ARM's Site Operations Staff at the Southern Great Plains Site, particularly that provided by Dan Nelson, Craig Webb and Rod Soper. Support for one of the authors, Q. Min, came from U.S. Department of Energy/ARM Program grant DE-FG02-03ER63531. The other authors were supported, in part, by the Atmospheric Science Research program of the U. S. Department of Energy, under Contract No. DE-AC02-98CH10886.

References

Bohren, C.F., J.R. Linskens and M.E. Churma, 1995: At what optical thickness does a cloud completely obscure the sun? J. Atmos. Sci., **53**, 1257-1259.

Crewell, S., and U. Löhnert, 2003: Accuracy of cloud liquid water path from ground-based microwave radiometer- 2. Sensor accuracy and synergy. Radio Sci., 38. 8042, doi:10.1029/2002RS002634.

Devore, J.G., A.T. Stair, A. LePage, D. Rall, J. Atkinson , D. Villanucci, S.A. Rappaport, P.C. Joss, and R.A. McClatchey, 2009. Retrieving properties of thin clouds from solar aureole measurements. JTech., 26, 2531-2548. DOI:10.1175/2009JTECHA1289.1

Dubovik, O. and M.D. King, 2000: A flexible inversion algorithm for retrieval of aerosol optical properties from sun and sky radiance measurements. J. Geophys. Res., **105**, 20,673-20,696.

Hansen, J.E., and L.D. Travis, 1974. Light scattering in planetary atmospheres, Space Sci. Rev., 16, 527-610.

Harrison, L. C., J. Michalsky, and J. Berndt, 1994: Automated multifilter rotating shadowband radiometer: An instrument for optical depth and radiation measurements. *Appl. Opt*., **33**, 5118-5125.

Hu, Y.X. and K. Stamnes, 1993. An accurate parameterization of the radiative properties of water clouds suitable for use in climate models, J. Climate, 6, 728-742.

Kaufman, Y.J., A. Gitelson, A. Karnieli, E. Ganor, R.S. Fraser, T. Nakajima, S. Mattoo, and B.N. Holben, 1994: Size distribution and scattering phase function of aerosol particles retrieved from sky brightness measurements, J. Geophys. Res., **99**(D5), 10341-10356.

Liljegren, J.C., and B.M. Lesht, 1996: Measurements of integrated water vapor and cloud liquid water from microwave radiometer at the DOE ARM cloud and radiation testbed in the Southern Great Plains. *Proc. Int. Geoscience Remote Sensing Symp*., Lincoln, NB, IGARSS, 1675-1677.

Marchland, R., T. P. Ackerman, E. R. Westwater, S. A. Clough, K. Cady-Periera, and J. C. Liljegren, 2003: An assessment of microwave absorption models and retrievals of cloud liquid water using clear-sky data, J. Geophys. Res, 108(D24), **4773**, doi:10.1029/2003JD003843.Miller, M.A., M.J. Bartholomew, and R.M. Reynolds, 2004: The accuracy of marine shadow-band measurements of aerosol optical thickness and Angstrom exponent. *J. Atmos. Ocean. Tech.*, **21**, 397-409.

Miller, M.A., K. Knobelspiesse, R. Frouin, M. J. Bartholomew, R. M. Reynolds, C. Pietras, G. Fargion, P. Quinn, and F. Thieuleux, 2005: Analysis of shipboard aerosol optical thickness measurements from multiple sunphotometers aboard the R/V Ronald H. Brown during the Aerosol Characterization Experiment – Asia." *Appl. Opt.*, **44**, 3805-3820.

Min, Q., E. Joseph, and M. Duan, 2004: Retrievals of thin cloud optical depth from a multifilter rotating shadowband radiometer, J. Geophys Res., **109**(D02201), doi:10.1029/2003JD003964.

Min, Q., and M. Duan , 2005: Simultaneously retrieving cloud optical depth and effective radius for optically thin clouds, *J. Geophys. Res.*, **110**(D21201), doi:10.1029/2005JD006136.

Nakijima, T, M. Tanaka and T. Yamauchi, 1983: Retrieval of the optical properties of aerosols from aureole and extinction data. Appl. Optics, **22**, 2951-2959.

Reynolds, M.R., M.A. Miller, and M.J. Bartholomew, 2001: Design, operation, and calibration of a fast-rotating, shadowband spectral radiometer for marine applications. *J. Atmos. Ocean. Tech*., **18**(2), 200–214.

Ritter, J.M., and K.J. Voss, 2000: A new instrument for measurement of the solar aureole radiance distribution from unstable platforms, J. Atmos. Oceanic Technol. 17, 1040-1048.

Sengupta, M., E.E. Clothiaux, T.P. Ackerman, S. Kato, and Q. Min, 2003. Importance of accurate liquid water path for estimation of solar radiation in warm boundary layer clouds: An observational study. J. Climate, 16,2997-3009.

Turner, D.D., S.A. Clough, J.C. Liljegren. E.E. Clothiaux, K. Cady-Pereira, K.L. Gaustad. 2007a: Retrieving liquid water path and precipitable water vapor from the Atmospheric Radiation Measurement (ARM) microwave radiometers, IEEE Transactions on Geosciences and Remote Sensing, **45**, 3680-3690.

Turner, D.D., A.M. Vogelmann, R.T. Austin, J.C. Barnard, K. Cady-Pereira, J.C. Chiu, S.A. Clough, C. Flynn, M.M. Khaiyer, J. Liljegren, K. Johnson, B. Lin, C. Long, A. Marshak, S.Y. Matrosov, S.A. McFarlane, M. Miller, Q. Min, P. Minnis, W. O'Hirok, Z. Wang and W. Wiscombe. 2007b: Thin liquid water clouds: Their importance and our challenge. BAMS, **88**, 117-190.

Yin, B., Q. Min, M. Duan, M.J. Bartholomew, A.M. Vogelmann, and D.D. Turner: Retrievals of cloud optical depth and effective radius from a thin-cloud rotating shadowband radiometer (TCRSR), submitted to Journal of Geophysical Research.

Westwater, E.R., Y. Han, M.D. Shupe, and S. Matrosov, 2001: Analysis of the integrated cloud liquid and precipitable water vapor retrievals from microwave radiometers during the Surface Heat Budget of the Arctic Ocean project. J. Geophys. Res., 106, 32 019-32 030.

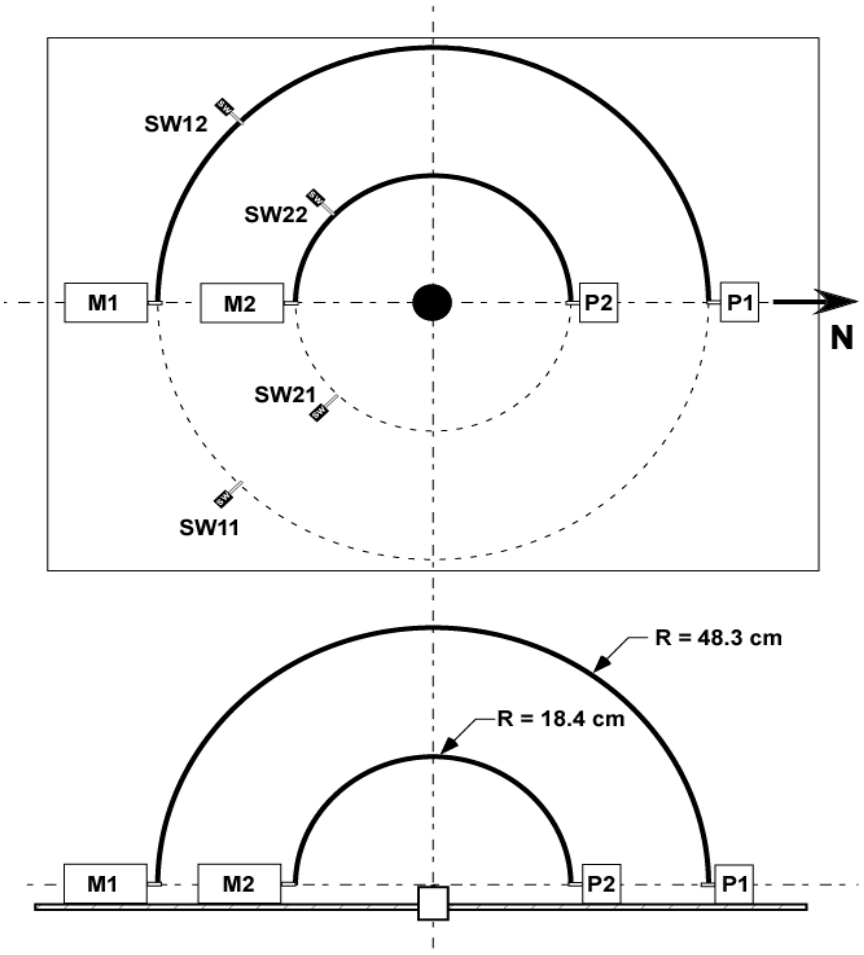

Figure 1: TCRSR Schematic. (Top) Overhead view looking down on the TCRSR with the MFRSR diffuser puck in the center. The outer and inner bands, respectively numbered 1 and 2, denote the 2º and 5º occultations. Each band is driven by a motor, M, at the left and have a pivot, P, at the right. The limit switches at opposite ends of the sweeps are labeled SWij, where i is the band (1 or 2 corresponding to the 2º or 5º band) and j is the limit position (1 or 2 corresponds to forward or reverse). (Bottom) Side view of the TCRSR. The final radii of the outer and inner bands are respectively, 48.3 and 18.4 cm and the width of both bands is 1.8 cm. This yields occultation angles of 2.13º and 5.6º. The diameter of the diffuser at the center is 0.81 cm. The MFRSR head is standard with one broadband channel and six 10-nm-wide narrowband channels nominally centered at 415, 500, 615, 673, 870 and 940 nm.

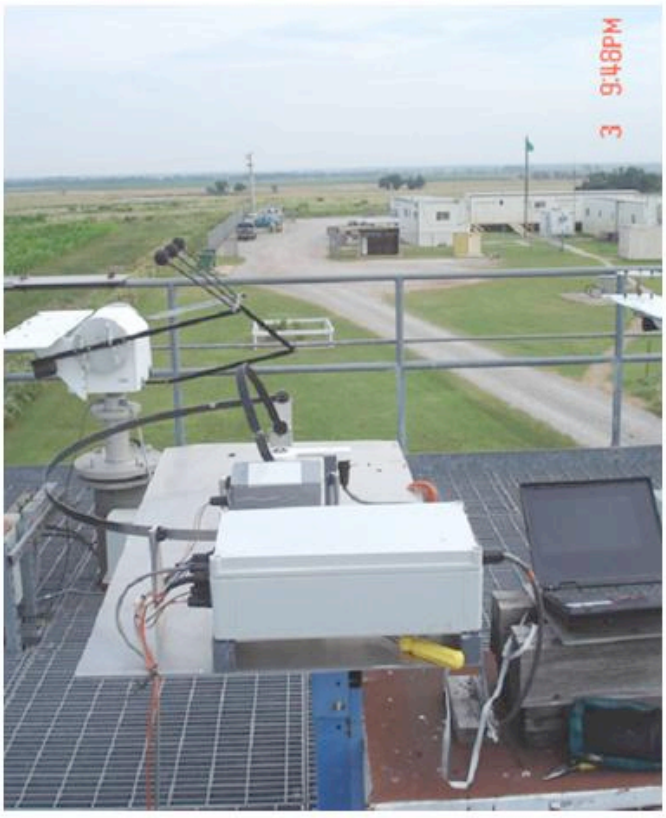

Figure 2: The TCRSR on the roof of ARM's Radiometer Calibration Facility at the Southern Great Plains Site. The control data unit is housed inside the white box in the foreground. The 2° band is in the full reverse position and the 5° band is rotating in the reverse direction. The instrument axis (north reference) is forward in this photo toward the horizon. A tracking device also can be seen just above and left of the TCRSR and the ARM Climate Research Facility offices appear top right.

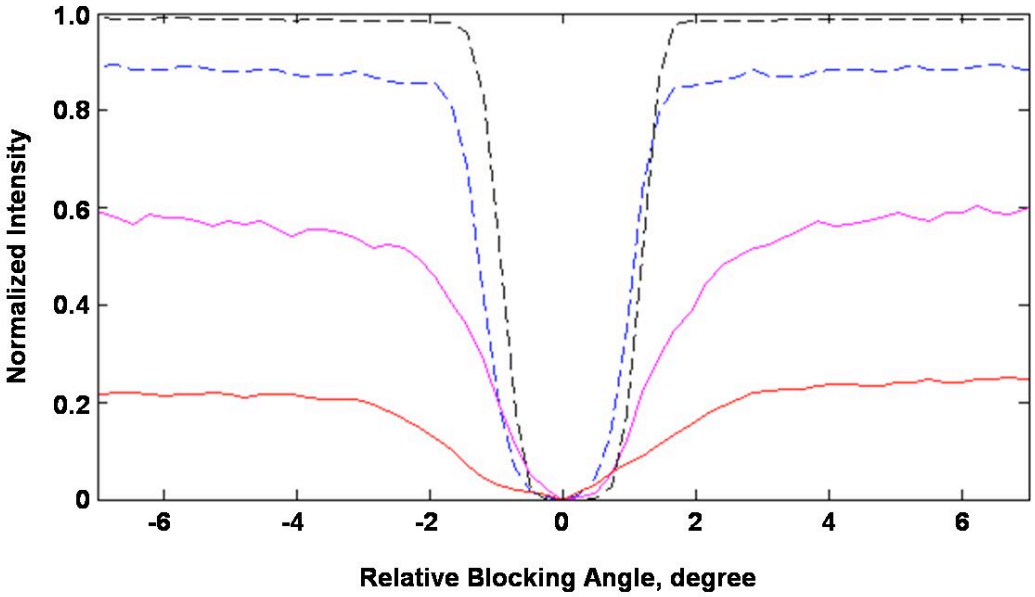

Figure 3: Examples of normalized sweeps for different sky conditions observed at 500 nm. The curves extend approximately ± 7° from the solar disk and were normalized for their minima to coincide at zero. Shown are two different warm thin clouds (solid red and magenta lines), an ice cloud case (dashed blue line) and a clear sky case (dashed black line). The warm cloud and ice cloud results are from July 3, 2008 at 16:21:18, 16:36:32, and 17:40:06 respectively. The clear-sky case is from July 2, 2008 at 17:11:52.

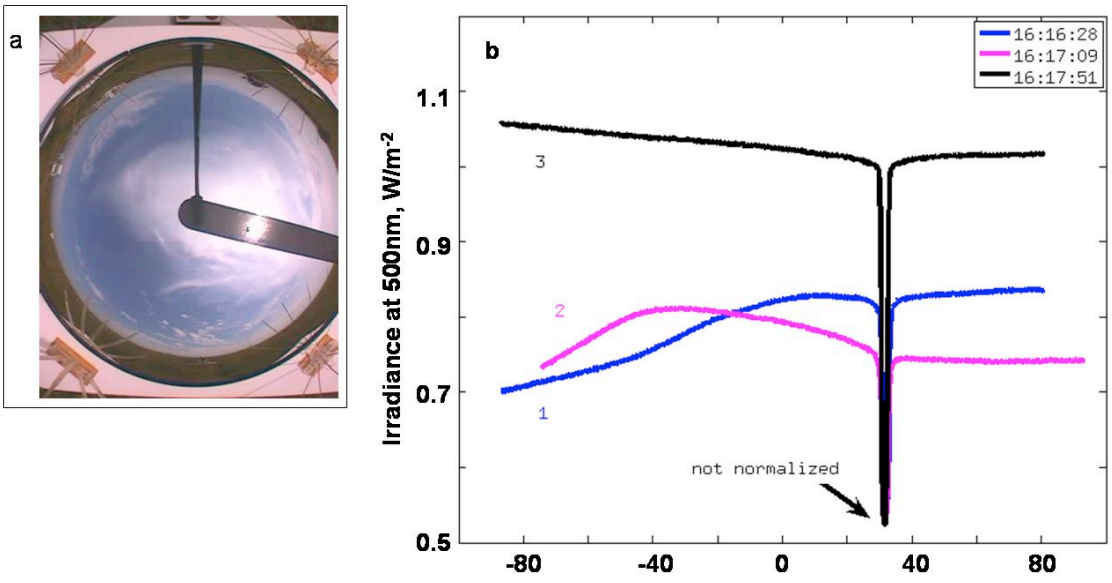

Figure 4: Consecutive TCRSR sweeps (b) observed on July 3, 2008. The relevant Total Sky Imager image (a) is shown to the left. The sweeps plotted in (b) illustrate the high degree of variability in the overall shape of the scans which could cause variations in typical hemispheric diffuse flux measurements. The same depth of the un-normalized dips, however, indicates that a similar optical depth would be retrieved.

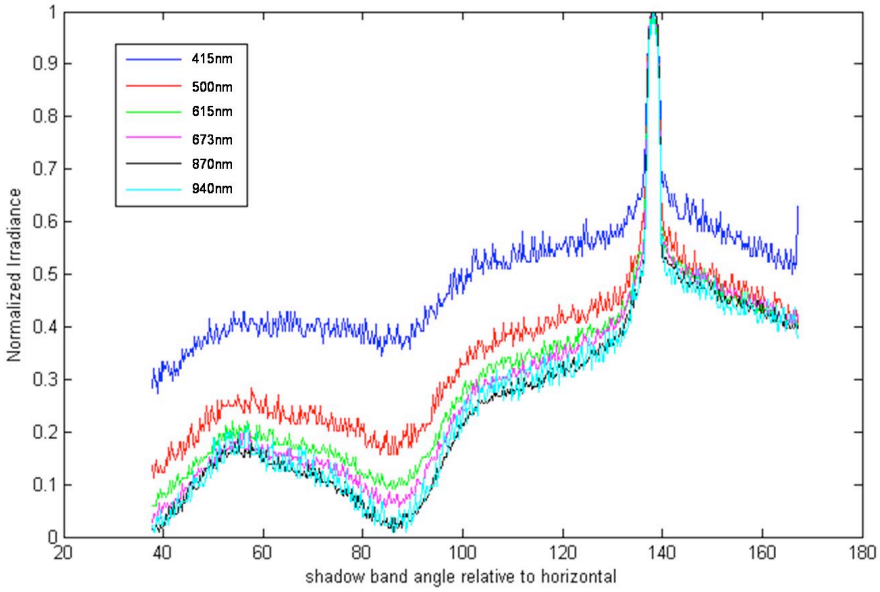

Figure 5: Scans (unblocked minus blocked) from all six narrow band channels (measured simultaneously) during a thin fog episode observed at Brookhaven National Laboratory on October 10, 2007 at 13:33:22 UTC. Each scan has been normalized by its maximum value. The maximum values contain the forward scattering lobe of the solar aureole plus the direct solar beam. Note the small variability relative to the signal magnitude, as well as the consistency in shape among the six channels.

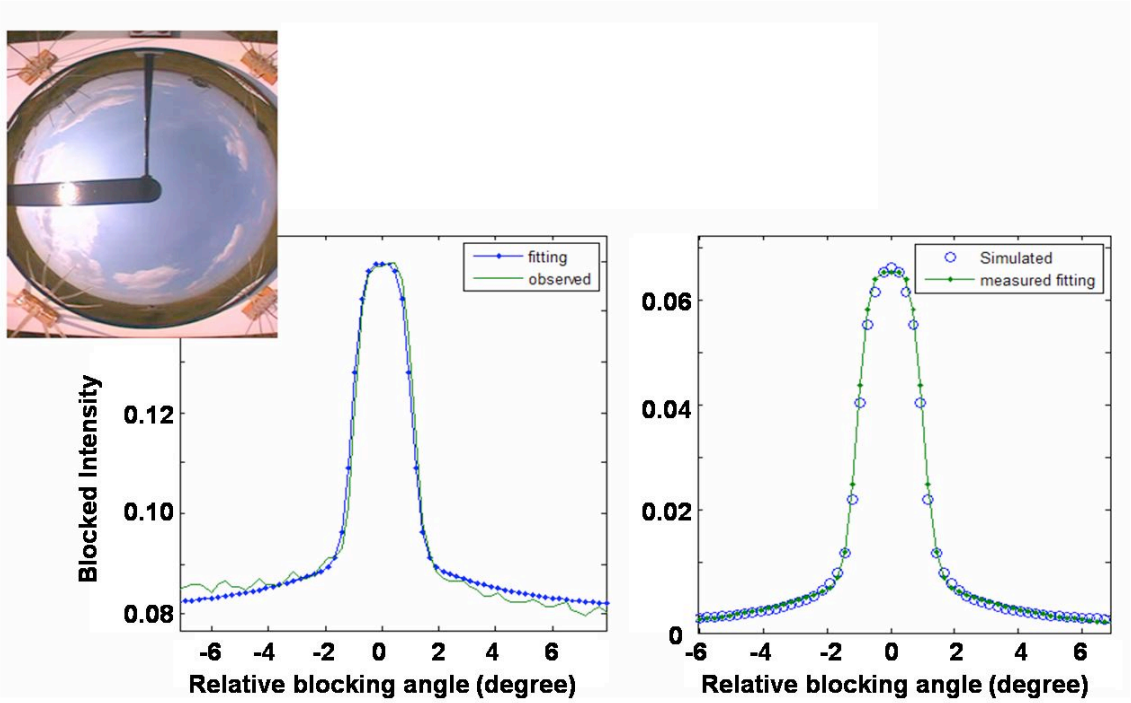

Figure 6: A sample retrieval for a case from July 3, 2008 at 22:02:20 UTC. (Top) Image from the total sky imager (TSI), showing the broken cloud field present at the time of the retrieval. The retrieval applies to the solar disk that is shadowed by the TSI shadowband. (Left) For retrieval stability, the observed unblocked-minus-blocked scan (green) is first smoothed (blue dots). (Right) Comparison of the simulation (blue circles) that best matches the shape of the smoothed result. The retrieved optical depth and Re are, respectively, 1.8 and 8 μm.